Mon. Not. R. Astron. Soc. **266,** 597–608 (1994)

Magnetic field evolution with Hall drift in neutron stars

Tsuguya Naito and Yasufumi Kojima
Department of Physics, Tokyo Metropolitan University, Hachiohji, Tokyo 192-03, Japan

Accepted 1993 August 6. Received 1993 June 17; in original form 1992 October 16

ABSTRACT

The role of the Hall current in plasma physics is studied in a model of neutron star magnetic fields. We calculate the evolution of the neutron star magnetic field with and without the Hall current effect. In our model, it is assumed that the magnetic field is confined to the crust and that the field dissipates through ohmic decay. The decay rates are expected to increase with the multipole moments if there is no Hall current and the dipole field is likely to survive. The presence of the Hall current causes coupling among the different modes, and the energy is transferred among them. We find that the dipole magnetic field does not always survive, and the decay features depend on the configuration of the fields. We speculate that some old neutron stars such as gamma-ray bursters may have strong, disordered-surface magnetic fields, but a weak dipole field.

Key words: magnetic fields – MHD – stars: magnetic fields – stars: neutron.

1 INTRODUCTION

A variety of magnetic fields have been observed in different types of neutron star. The field strength at the surface is $B_s < 10^9$ G in X-ray bursters, $B_s \sim 10^8$–10^{10} G in millisecond pulsars and $B_s \sim 10^{12}$ G in radio pulsars, X-ray pulsars and gamma-ray bursters. Because the ages of these types of object are different, it has been proposed that the magnetic fields evolve with time. Some observations support this theory, while others do not. This study has been performed to clarify the mechanism, if any, of the evolution of magnetic fields.

The evolutionary model was first suggested as a result of statistical analyses of radio pulsars. If the radio pulsars spin down as a result of magnetic dipole radiation, their magnetic strengths and their ages can be estimated from the observed pulse period and spin-down rate. Their field strengths are typically $B_s \sim 10^{12}$ G and their ages peak at a few million years (e.g. see review by Manchester & Taylor 1977). Ostriker & Gunn (1969) suggested that the magnetic field of pulsars must decay exponentially on a time-scale $\tau \sim 10^7$ yr to fit the observational data. More recent detailed statistical analyses indicate that the fields decay on a time-scale of $(5–9)\times 10^6$ yr (Lyne, Manchester & Taylor 1985) or $(8–18)\times 10^6$ yr (Narayan & Ostriker 1990). A different interpretation is possible, however, even using the same data. Lamb (1992) concluded that the evidence supporting magnetic field evolution is not conclusive because of the large error bars.

Recently, a mechanism for magnetic field evolution was proposed that may relate to binary systems. X-ray pulsars are young ($\sim 10^7$ yr) and have strong magnetic fields ($\sim 10^{12}$ G), while X-ray bursters are old ($\sim 10^{10}$ yr) and have weak fields ($< 10^9$ G). The recently discovered millisecond pulsars are recycled neutron stars ($\sim 10^{10}$ yr) and have relatively small magnetic fields (10^8–10^{10} G). However, it is difficult to reconcile this class of neutron stars with such a simple magnetic field decay model. Taam & van den Heuvel (1986) speculated that the magnetic field decays until $B_s \sim 3\times 10^9$ G with a time constant $\sim 10^7$ yr, but the field decay rates become slower at $B_s < 3\times 10^9$ G in a binary system. Another mechanism was suggested by Shibazaki et al. (1989). They proposed that mass accretion causes neutron star magnetic field decay. The neutron stars in binary systems suffer mass accretion from their companion stars, and their magnetic fields may evolve with time. On the other hand, gamma-ray bursts, which may be old isolated neutron stars, have still strong magnetic fields ($\sim 10^{12}$ G), as inferred from cyclotron lines in their spectra (Murakami et al. 1988). Nevertheless, there are counter-examples to such a viewpoint. Detailed studies of the evolutionary scenarios for the binary X-ray pulsars Her X-1 and 4U1626 − 67 have suggested that these neutron stars are $\geq 10^8$ yr old and have undergone large mass accretion, but still retain strong magnetic fields ($\sim 10^{12}$ G) (Verbunt, Wijers & Burm 1990). These stars may show no magnetic field decay.

On the other hand, the theoretical evolutionary models depend on factors such as the magnetic field configuration and dissipation mechanisms. Ostriker & Gunn (1969) also suggested a theoretical model that explains the observed exponential decay. If a star has a radius R and uniform electrical conductivity σ, its dipole magnetic field decays by ohmic dissipation with a time-scale $\tau_D = 4R^2\sigma/\pi c^2$ (Lamb 1883). They roughly estimated the conductivity as $\sigma \sim 0.4 \times 10^{22}$ s^{-1} and concluded that the characteristic time-scale is $\tau_D \sim 4 \times 10^6$ yr. Baym, Pethick & Pines (1969b) determined the conductivity in the neutron star core, obtaining a value of $\sigma \sim 0.4 \times 10^{29}$ s^{-1}, and therefore a time-scale $\tau_D \sim 10^{13}$ yr. This time-scale greatly exceeds the Hubble time – in other words, there is no significant magnetic field decay. If the magnetic field penetrates to the central core, ohmic diffusion becomes ineffective. Some authors (Jones 1987, 1988; Harrison 1991) therefore sought some process to expel the magnetic field from the central core, such as buoyancy force, Magnus force or viscous force, but none of them changes effectively the magnetic field in a Hubble time.

If the field is localized in the crust, ohmic dissipation may cause a change in the magnetic field. Sang & Chanmugam (1987) calculated evolutionary models of the magnetic field using a position-dependent conductivity. Their results show that the magnetic fields decay non-exponentially. Urpin & Muslimov (1992) considered the effect of the thermal history of the neutron star. They showed that the field decreases rapidly during the first 10^6–10^7 yr, but the field decay stops after the star cools down and the conductivity increases.

In this paper, we examine the effect of the Hall current in Ohm's law, which was ignored in the previous evolutionary calculations but cannot be neglected under some conditions. The Hall current does not result in dissipation, but rather in advection of the magnetic field. It is the non-linear term of the magnetic field. When we perform multipole expansion of the field, the Hall current couples the dipole field to higher modes. Without this coupling, the time evolution of the field can be separated into individual multipole modes. The higher modes decay faster than the lower modes (Wendell, Van Horn & Sargent 1987; Sang & Chanmugam 1987, 1990; see also Section 3), and the dipole component survives long after the other components have disappeared. If there are couplings among the multipole moments, the energy of the dipole field is converted to that of higher modes. Magnetic field decay of the dipole moment may be enhanced through the decay of the higher modes. If this mechanism does in fact take place in a neutron star, the star will have small dipole magnetic fields and strong chaotic magnetic fields. Krolik (1991) pointed out the possibility that the magnetic fields of millisecond pulsars may be given by $B_s \sim 10^{12}$ G if the multipole moments with $l \geq 3$ dominate, and he further speculated that the gamma-ray bursters may have a similar magnetic field configuration. Moreover, the observation that gamma-ray bursts show no pulse feature may support such a magnetic field configuration.

In Section 2 we briefly review the plasma physics in a neutron star, especially in its crust, and derive the generalized ohmic law from magnetohydrodynamics (MHD). Section 3 presents a new model of magnetic field evolution. In order to examine the effect of the Hall current, we adopt rather simplified models. The magnetic fields are assumed to be axially symmetric and confined outside the core, and the electrical conductivity is constant in space and time. We use the multipole expansion to solve the evolution of the magnetic fields. The numerical methods for some cases, and their results, are given in Section 4. Section 5 is devoted to a discussion.

2 PLASMA PHYSICS IN A NEUTRON STAR

2.1 Superconducting core

As a result of the effective interaction between isolated protons, protons in the central core of a neutron star are in an $^1S_0$ pairing state (Chao, Clark & Yang 1972). Since the London penetration depth of the proton pair, $\lambda_L \sim 10^{-11}$ cm, exceeds the coherence length of $\xi \sim 10^{-12}$ cm, the proton liquid is a type II superconductor (Pines & Alpar 1985; Harrison 1991). The critical magnetic fields in the central core, H_{c1} and H_{c2}, have the values

$$H_{c1} \sim \frac{\Phi_0}{\pi\lambda_L^2} \sim 3 \times 10^{14} \text{ G}, \tag{1}$$

$$H_{c2} \sim \frac{\Phi_0}{\pi\xi^2} \sim 3 \times 10^{16} \text{ G}, \tag{2}$$

where $\Phi_0 = hc/2e = 2 \times 10^{-7}$ G cm^2 is a fluxoid (a quantized flux tube). When $B < H_{c1}$, the expulsion of the field occurs as a result of the Meissner effect, whereby the magnetic field lines are pushed out of the superconducting core. When $H_{c1} < B < H_{c2}$, the field can penetrate the superconductor as a fluxoid with characteristic radius ξ. When $B > H_{c2}$, the superconducting state is destroyed so that protons return to their normal degenerate state (Harrison 1991).

We should consider two possible magnetic field configurations: penetrating or not penetrating to the core of a star. Since a high conductivity of the electron gas causes a great delay of the expulsion (Baym, Pethick & Pines 1969a), the magnetic field can exist in a type II superconductor as vortex lines (Alpar et al. 1984a; Alpar, Langer & Sauls 1984b). If the magnetic field is

created in the central core before the star has cooled below the transition temperature to the superconducting state, the field continues to penetrate to the core. In this case, ohmic dissipation is too small to influence the magnetic field because of the high conductivity. Several processes for the expulsion of the magnetic field from the central core, such as buoyancy force, Magnus force and viscous force, have been discussed in various papers (Jones 1987, 1988; Harrison 1991), but none of them effectively changes the magnetic field in a Hubble time. On the other hand, if the magnetic field is created in the crust as a result of thermodynamic effects (Blandford, Applegate & Hernquist 1983; Urpin, Levshakov & Yakovlev 1986) after the transition and $B_{\rm core} < H_{\rm c1}$, the field cannot enter the core as a result of the Meissner effect. In this case, ohmic dissipation may cause a change in the magnetic field, with a time-scale characterized by the electrical conductivity (Sang & Chanmugam 1987, 1990; Urpin & Muslimov 1992).

2.2 Magnetohydrodynamics in the crust

In this section, we investigate plasma physics in a neutron star crust which consists of free electrons, free neutrons and neutron-rich nuclei. The electrons comprise a highly degenerate relativistic gas. The free neutrons are in a superfluid state. Most of the heavy nuclei form a lattice, while some exist freely. We consider only two equations of motion for electrons and nuclei, because the electrons interact only with normal particles, i.e. nuclei, in the sea of superfluid neutrons. The effect of collisions between normal particles and superfluid neutrons is negligible compared to the Coulomb interaction. The electrons and the nuclei are subject to the Lorentz, pressure gradient, gravitational and collisional forces. In a strong magnetic field, we can neglect the nucleus–nucleus and electron–electron collisions because of cyclotron motion (Chen 1986). We also ignore the shear stress tensor here. Thus the equations of motion for nuclei and electrons can be written as

$$Mn_{\rm n}\frac{\partial \boldsymbol{v}_{\rm n}}{\partial t} = Zen_{\rm n}\left(\boldsymbol{E}+\frac{\boldsymbol{v}_{\rm n}\times\boldsymbol{B}}{c}\right) - \nabla P_{\rm n} + Mn_{\rm n}\boldsymbol{g} + \boldsymbol{\Pi}_{\rm ne}, \tag{3}$$

$$mn_{\rm e}\frac{\partial \boldsymbol{v}_{\rm e}}{\partial t} = -en_{\rm e}\left(\boldsymbol{E}+\frac{\boldsymbol{v}_{\rm e}\times\boldsymbol{B}}{c}\right) - \nabla P_{\rm e} + mn_{\rm e}\boldsymbol{g} + \boldsymbol{\Pi}_{\rm en}, \tag{4}$$

where M and m are the masses of the nucleus and the electron respectively, and $n_{\rm n}$ ($n_{\rm e}$), $\boldsymbol{v}_{\rm n}(\boldsymbol{v}_{\rm e})$ and $P_{\rm n}(P_{\rm e})$ are the number density, velocity and pressure of the nucleus (electron). The collision terms, $\boldsymbol{\Pi}_{\rm ne}$ and $\boldsymbol{\Pi}_{\rm en}$, represent the momentum gain of the nuclei per unit time and per unit volume caused by collisions with electrons, and vice versa.

We assume the existence of a single species of nucleus with charge number Z. The charge neutrality is given by

$$Zn_{\rm n} = n_{\rm e} = n. \tag{5}$$

Since the collision terms are proportional to the charge of the particles, their number density and their relative velocity, we can write

$$\boldsymbol{\Pi}_{\rm ne} = \frac{1}{\sigma_{\rm n}} Ze^2 n_{\rm n} n_{\rm e}(\boldsymbol{v}_{\rm e}-\boldsymbol{v}_{\rm n}),$$

$$\boldsymbol{\Pi}_{\rm en} = \frac{1}{\sigma_{\rm e}} Ze^2 n_{\rm e} n_{\rm n}(\boldsymbol{v}_{\rm n}-\boldsymbol{v}_{\rm e}). \tag{6}$$

This is the definition of electrical conductivity. The conductivities of the nucleus and the electron are related by

$$\frac{1}{Z}\sigma_{\rm n} = \sigma_{\rm e} = \sigma. \tag{7}$$

Therefore, using σ and n, we have

$$\boldsymbol{\Pi}_{\rm en} = -Z\Pi_{\rm ne} = \frac{1}{\sigma} e^2 n^2(\boldsymbol{v}_{\rm n}-\boldsymbol{v}_{\rm e}). \tag{8}$$

From the definition of the collision term, we obtain

$$\frac{1}{\sigma} e^2 n^2(\boldsymbol{v}_{\rm n}-\boldsymbol{v}_{\rm e}) = p_{\rm F} n_{\rm e}\frac{1}{\tau_{\rm tr}}, \tag{9}$$

where p_F is the Fermi momentum of the electrons, τ_{tr} is the transition time of electron–nucleus collisions and σ is the electrical conductivity. We assume that σ is constant in the crust and takes a value of $\sigma \sim 4.7 \times 10^{25}\ \mathrm{s}^{-1}$ (Baym et al. 1969b; Ewart, Guyer & Greenstein 1975; Flowers & Itoh 1976; see also Section 4.2).

It is more convenient to deal with a linear combination of each velocity than with $\boldsymbol{v}_n$ and $\boldsymbol{v}_e$, because $\boldsymbol{v}_n - \boldsymbol{v}_e$ is related to the electric current and $Mn_n\boldsymbol{v}_n + mn_e\boldsymbol{v}_e$ is related to motion of the centre of mass. The linear combination describes the plasma as a single fluid. This method is called the MHD single-fluid approximation. We define the mass density ρ, velocity of centre of mass $\boldsymbol{v}$ and current density $\boldsymbol{j}$ as follows:

$$\rho = n_n M + n_e m = n\left(\frac{M}{Z} + m\right), \tag{10}$$

$$\boldsymbol{v} = \frac{1}{\rho}(Mn_n\boldsymbol{v}_n + mn_e\boldsymbol{v}_e) = \frac{\frac{M}{Z}\boldsymbol{v}_n + m\boldsymbol{v}_e}{\frac{M}{Z} + m}, \tag{11}$$

$$\boldsymbol{j} = Zen_n\boldsymbol{v}_n - en_e\boldsymbol{v}_e = en(\boldsymbol{v}_n - \boldsymbol{v}_e). \tag{12}$$

From the addition of equations (3) and (4), we have

$$\rho\frac{\partial \boldsymbol{v}}{\partial t} = \frac{\boldsymbol{j}\times\boldsymbol{B}}{c} - \nabla P + \rho\boldsymbol{g}, \tag{13}$$

where $P = P_n + P_e$. This is the single-fluid equation of motion. From the subtraction of equations (3) and (4), we obtain

$$\boldsymbol{E} + \frac{\boldsymbol{v}\times\boldsymbol{B}}{c} = \frac{1}{\sigma}\boldsymbol{j} + \frac{1}{en}\frac{\boldsymbol{j}\times\boldsymbol{B}}{c} - \frac{1}{en}\nabla P_e, \tag{14}$$

where $m \ll M$. This is the generalized version of Ohm's law. We note the Hall current term $\boldsymbol{j}\times\boldsymbol{B}$, which both equations (13) and (14) involve. When the neutron star system lies in an equilibrium state $\partial\boldsymbol{v}/\partial t = 0$, the equation of motion (13) becomes

$$\frac{\boldsymbol{j}\times\boldsymbol{B}}{c} - \nabla P + \rho\boldsymbol{g} = 0. \tag{15}$$

In the radial component of this equation, the pressure gradient force and the gravitational force dominate, so that we neglect the first term, and

$$-\nabla_r P + \rho g_r = 0. \tag{16}$$

Since the electron pressure and the gravitational force are highly isotropic, the toroidal component of $\boldsymbol{j}\times\boldsymbol{B}$ balances the fluctuations in the nuclear pressure gradient (Jones 1988):

$$\frac{(\boldsymbol{j}\times\boldsymbol{B})}{c} - \delta(\nabla P) = 0. \tag{17}$$

Since the magnitude of these fluctuations cannot be estimated easily, we do not substitute the relation (17) into equation (14). In the next section we will treat the Hall current term directly in Ohm's law.

3 MODEL OF MAGNETIC FIELD EVOLUTION

3.1 Time evolution equation

For convenience, we move in the frame corotating with the neutron star, so that the velocity $\boldsymbol{v}$ vanishes. Thus the generalized version of Ohm's law is written as

$$\boldsymbol{E} = \frac{1}{\sigma}\boldsymbol{j} + \frac{1}{en}\frac{\boldsymbol{j}\times\boldsymbol{B}}{c} - \frac{1}{en}\nabla P_e. \tag{18}$$

Faraday's induction equation and Ampère's equation are

$$c\nabla\times\boldsymbol{E}=-\frac{\partial\boldsymbol{B}}{\partial t} \tag{19}$$

and

$$c\nabla\times\boldsymbol{B}=4\pi\boldsymbol{j}. \tag{20}$$

In equation (20), the displacement current ($\partial\boldsymbol{E}/\partial t=0$) is neglected. Substituting equations (18) and (20) into equation (19), we can obtain the equation governing the time evolution of the magnetic field,

$$\frac{\partial\boldsymbol{B}}{\partial t}=-\nabla\times\left(\frac{c^2}{4\pi\sigma}\nabla\times\boldsymbol{B}\right)-\nabla\times\left[\frac{c}{4\pi ne}(\nabla\times\boldsymbol{B})\times\boldsymbol{B}\right]. \tag{21}$$

If the second term of the right-hand side can be neglected, this equation is reduced to the form already used by many authors (Sang & Chanmugam 1987; Jones 1988; Urpin & Muslimov 1992).

Next we consider the conditions under which the Hall current becomes important. Comparing the magnitudes of the first and second terms on the right-hand side of equation (21), we cannot neglect the second term if

$$B\geq\frac{nec}{\sigma}\sim 10^{11}\,\sigma_{25}^{-1}\ \mathrm{G}, \tag{22}$$

where $\sigma_{25}=10^{25}\ \mathrm{s}^{-1}$. However, the Hall drift does not work under a specific field configuration. For example, if the toroidal field never appears, the evolution of the poloidal field can be described only by the first term (ohmic dissipation).

3.2 Expansion by Legendre polynomials

We assume an axially symmetric configuration of the magnetic field: $\boldsymbol{B}\equiv\boldsymbol{B}(t, r, \theta)$ using spherical coordinates. We expand the vector potential $\boldsymbol{A}$ by the set of Legendre polynomials $P_l(\cos\theta)$, as

$$\begin{aligned}
A_r(t, r, \theta)&=-\sum_{l=1}^{\infty}\frac{g_l(t, r)}{l(l+1)}P_l(\cos\theta),\\
A_\theta(t, r, \theta)&=-\frac{1}{r}\sum_{l=1}^{\infty}\frac{h_l(t, r)}{l(l+1)}\frac{\partial P_l(\cos\theta)}{\partial\theta},\\
A_\varphi(t, r, \theta)&=-\frac{1}{r}\sum_{l=1}^{\infty}\frac{b_l(t, r)}{l(l+1)}\frac{\partial P_l(\cos\theta)}{\partial\theta},
\end{aligned} \tag{23}$$

where the summations run from $l=1$, not from $l=0$, because of the absence of a monopole magnetic field. The functions $g_l(t, r)$, $h_l(t, r)$ and $b_l(t, r)$ are expansion coefficients which depend on time and radius.

From $\boldsymbol{B}=\nabla\times\boldsymbol{A}$, the poloidal magnetic field is

$$\begin{aligned}
B_r(t, r, \theta)&=\frac{1}{r^2}\sum_{l=1}^{\infty}b_l(t, r)P_l(\cos\theta),\\
B_\theta(t, r, \theta)&=\frac{1}{r}\sum_{l=1}^{\infty}\frac{1}{l(l+1)}\frac{\partial b_l(t, r)}{\partial r}\frac{\partial P_l(\cos\theta)}{\partial\theta},
\end{aligned} \tag{24}$$

where we have used a differential relation for the Legendre polynomial (see Appendix). On the other hand, the toroidal magnetic field is described by

$$B_\varphi(t, r, \theta)=-\frac{1}{r}\sum_{l=1}^{\infty}\frac{1}{l(l+1)}\left[\frac{\partial h_l(t, r)}{\partial r}-g_l(t, r)\right]\frac{\partial P_l(\cos\theta)}{\partial\theta}=-\frac{1}{r}\sum_{l=1}^{\infty}\frac{1}{l(l+1)}f_l(t, r)\frac{\partial P_l(\cos\theta)}{\partial\theta}, \tag{25}$$

where we have defined the function $f_l(t, r)$ as

$$f_l(t, r)=\frac{\partial h_l(t, r)}{\partial r}-g_l(t, r). \tag{26}$$

Substituting equations (24) and (25) into (21) and using the orthogonality condition, we can obtain the time-evolution functions:

$$\frac{\partial b_l}{\partial t}=\alpha\left(\frac{\partial^2}{\partial r^2}-\frac{\lambda}{r^2}\right)b_l+\frac{\beta}{r^2}\sum_{l_1\,l_2}S_{l_1l_2l}\left(f_{l_1}\frac{\partial b_{l_2}}{\partial r}-b_{l_1}\frac{\partial f_{l_2}}{\partial r}\right), \tag{27}$$

$$\frac{\partial f_l}{\partial t}=\alpha\left(\frac{\partial^2}{\partial r^2}-\frac{\lambda}{r^2}\right)f_l-\frac{\partial\alpha}{\partial r}\frac{\partial f_l}{\partial r}+\frac{1}{r^2}\sum_{l_1\,l_2}\left\{S_{l_1l_2l}\left(\frac{\partial\beta}{\partial r}-\frac{2\beta}{r}\right)(f_{l_1}f_{l_2}+b_{l_1}a_{l_2})\right.$$
$$\left.+\beta\left[(S_{l_1l_2l}+S'_{l_1l_2l})\frac{\partial b_{l_1}}{\partial r}a_{l_2}+S_{l_1l_2l}b_{l_1}\frac{\partial a_{l_2}}{\partial r}+(S_{l_1l_2l}+S'_{l_1l_2l})\frac{\partial f_{l_1}}{\partial r}f_{l_2}+S_{l_1l_2l}f_{l_1}\frac{\partial f_{l_2}}{\partial r}\right]\right\}, \tag{28}$$

where

$$\alpha=\frac{c^2}{4\pi\sigma},\qquad \beta=\frac{c}{4\pi ne},\qquad \lambda=l(l+1),\qquad \lambda_i=l_i(l_i+1), \tag{29}$$

and

$$a_l(t,r)=\alpha\frac{\partial^2 b_l(t,r)}{\partial r^2}-\frac{\lambda}{r^2}b_l(t,r). \tag{30}$$

S and S' indicate the integrals for the Legendre polynomials, which can be expressed by the Clebsch–Gordan coefficient, $C(l_1l_2l_3;m_1m_2m_3)$ (see Appendix):

$$S_{l_1l_2l}=\frac{2l+1}{2}\frac{1}{\lambda_1\lambda_2}\int_{-1}^{1}\mathrm{d}(\cos\theta)\frac{\partial P_{l_1}}{\partial\theta}\frac{\partial P_{l_2}}{\partial\theta}P_l=\sqrt{\frac{\lambda}{\lambda_2}}\,C(l_1l_2l;011)\,C(l_1l_2l;000),$$

$$S'_{l_1l_2l}=\frac{2l+1}{2}\frac{1}{\lambda_1\lambda_2}\int_{-1}^{1}\mathrm{d}(\cos\theta)P_{l_1}\frac{\partial P_{l_2}}{\partial\theta}\frac{\partial P_l}{\partial\theta}=\frac{2l+1}{2l_1+1}\frac{1}{\sqrt{\lambda_1\lambda_2}}\,C(ll_2l_1;011)\,C(ll_2l_1;000). \tag{31}$$

3.3 Effect of Hall current term

Equations (27) and (28) are time-developing functions of the poloidal and toroidal components, respectively. If the Hall current always vanishes, equation (27) becomes linear in terms of the magnetic field strength, so that different modes with spherical harmonic index l decay independently. For example, in the sphere with constant electrical conductivity, the field decays as

$$b_l(t,r)=\sum_{n=0}^{\infty}b_{ln}(r)\exp\left(-\frac{t}{\tau_{ln}}\right), \tag{32}$$

where the characteristic time-scale τ_{ln} is expressed by the zeros of the spherical Bessel function $j_l(x_{ln})=0$:

$$\tau_{ln}=\frac{4\pi R^2\sigma}{c^2x_{l-1\,n}^2}, \tag{33}$$

and where n is the number of nodes of the radial function. For the dipole case ($l=1$), we have

$$\tau_{ln}=\frac{4R^2\sigma}{\pi c^2(n+1)^2}. \tag{34}$$

In general,

$$\tau_{ln}>\tau_{l+1\,n}>\tau_{ln+1}. \tag{35}$$

The higher modes therefore decay faster (see also Wendell et al. 1987; Sang & Chanmugam 1987, 1990).

On the other hand, the Hall current term plays the role of a bridge between various modes (ls) of the magnetic field. We expect the Hall current term to transform the energy of the dipole field into that of the higher modes such as the quadra-component, etc.

The time-scale of this transition is estimated as

$$\tau_{\rm H} \sim \frac{4\pi neR^2}{cB} \sim 10^8 \left(\frac{B}{10^{11}\,{\rm G}}\right)^{-1} {\rm yr}. \tag{36}$$

3.4 Boundary conditions

From $\nabla \cdot \boldsymbol{B} = 0$, the normal component of the magnetic field, i.e. B_r, must be continuous. For the inner boundary there are two physically different conditions of $\boldsymbol{B}$: penetrating and not penetrating to the core, as seen in Section 2.1. The former condition indicates that $B_r(t,\, r = R_{\rm in}) =$ constant, where $R_{\rm in}$ is the radius of the central core. In the latter condition, the magnetic field is initially confined to the entire crust, without penetration into the central core. Hence $B_r(t,\, R_{\rm in}) = 0$. The tangential components, B_θ and B_φ, may be discontinuous due to the surface current. In this way, for the innermost boundary condition we only fix $B_r(t,\, R_{\rm in})$ to be a certain value, and do not specify B_θ and B_φ. Mathematically, this corresponds to the Dirichlet boundary condition for b_l, because B_r is given by b_l and B_θ by $\partial b_l/\partial r$ (see equation 24).

The boundary condition at the surface depends on the environment outside the star. We will examine two cases. One [case (i)] involves the condition where the star is isolated in a vacuum. The exterior magnetic field is described only by the poloidal field, i.e. $B_\varphi = 0$. In this case there is no surface current: $j_\varphi = 0$. The normal components of the field, B_r, should be continuous and the tangential components are also continuous at the surface. Thus the poloidal components, B_r and B_θ, should be matched to the multipole moments in a vacuum and the toroidal component, B_φ, goes to zero at the surface. In the other case considered [case (ii)], the star retains contact with the constant exterior magnetic fields, $B_\varphi \neq 0$, which are non-zero due to the accretion of matter in the binary system. In this case, B_r and B_θ connect smoothly to the values of the multipole moment, and B_φ goes to a fixed value.

Next, we consider the differences in energy between these two cases. The time variation of magnetic energy is given by

$$\frac{\partial W}{\partial t} = -\frac{1}{\sigma}\int_V \boldsymbol{j}\cdot\boldsymbol{j}\,{\rm d}V - \frac{c}{4\pi}\int_S (\boldsymbol{E}\times\boldsymbol{B})\cdot{\rm d}\boldsymbol{S}, \tag{37}$$

where W is the magnetic energy,

$$W = \frac{1}{8\pi}\int_V \boldsymbol{B}\cdot\boldsymbol{B}\,{\rm d}V. \tag{38}$$

The description (37) can be obtained irrespective of the Hall current in Ohm's law. The first term of the right-hand side exhibits energy dissipation as Joule heat. The second term expresses energy diffusion through the Poynting flux. If the radial component of $\boldsymbol{E}\times\boldsymbol{B}$ does not vanish at the stellar surface, the magnetic energy leaks out from the star. From Ohm's law (equation 18), we can see immediately that $(\boldsymbol{E}\times\boldsymbol{B})_r = 0$ means that $(\boldsymbol{j}\times\boldsymbol{B})_r = 0$. The conditions $j_\varphi = 0$ and $B_\varphi = 0$ at the surface ensure that $(\boldsymbol{j}\times\boldsymbol{B})_r = 0$. Case (i) above corresponds to $j_\varphi = B_\varphi = 0$, which means there is no Poynting flux, and hence the magnetic energy results only in a Joule heating. However, case (ii) means that the magnetic energy in the star can leak out to the outside plasma because $B_\varphi \neq 0$ at the surface.

4 NUMERICAL RESULTS

4.1 Method

In this subsection we briefly explain our numerical method. We use the finite difference method to solve equations (27) and (28). If there is no Hall current term, the basic equations become diffusion-type. We therefore apply the Crank–Nicolson scheme to the time evolution and the ohmic diffusion terms. That is, we replace the time and space differentiations for an arbitrary function $u(t, r)$ at t_k, r_j as follows:

$$\frac{\partial u}{\partial t} \to \frac{u_j^{k+1} - u_j^{k-1}}{2\Delta t},$$

$$\frac{\partial u}{\partial r} \to \frac{1}{2}\left(\frac{u_{j+1}^{k+1} - u_{j-1}^{k+1} + u_{j+1}^{k-1} - u_{j-1}^{k-1}}{2\Delta r}\right),$$

$$\frac{\partial^2 u}{\partial r^2} \to \frac{1}{2}\left(\frac{u_{j+1}^{k+1} - 2u_j^{k+1} + u_{j-1}^{k+1} + u_{j+1}^{k-1} - 2u_j^{k-1} + u_{j-1}^{k-1}}{4\Delta r^2}\right), \tag{39}$$

where $u_{j\pm l}^{k\pm l} = u(t_k \pm \Delta t, r_j \pm \Delta r)$. As shown in previous sections, the Hall current terms are non-linear in $b_l(t, r)$ and $f_l(t, r)$, so that we simply adopt explicit differencing for such terms. We replace them by the values at t_k, which are calculated by the staggered leapfrog method. Thus we have a numerical scheme with second-order accuracy in space and time. The stability of this scheme is guaranteed, if the non-linear terms are small; however, the scheme may become unstable if they are large. Therefore we limit our calculations to the case where ohmic dissipation dominates. The solutions under this restriction, however, will none the less represent certain properties of the Hall current.

4.2 Results

We take the standard values for a neutron star: that is, radius $R_s = 10$ km and mass $M = 1.4\ M_\odot$. The boundary between the crust and the central core is typically $r = R_0 = 0.9R_s$, i.e. the thickness is 1 km. Such a neutron star has a central density $\rho_c \geq 10^{14}$ g cm^{-3}, a crust density $\rho \simeq 10^{14}$–10^{13} g cm^{-3} (Shapiro & Teukolsky 1983), and a temperature $T \simeq 10^8$–10^9 K (Nomoto & Tsuruta 1987) at equilibrium. When the number density of electrons is a small percentage of that for neutrons, the electrical conductivity of the crust is $\sigma \simeq 4.7 \times 10^{25}$ s^{-1}. These values correspond to the time-scale of ohmic diffusion, $\tau_D \sim 10^8$ yr.

We perform the expansion by Legendre polynomials in equations (24) and (25) up to $l = 5$, but we find that the results for small l described below are almost unchanged even if we use a larger l_{max}, e.g. $l_{max} = 10$. Since we do not know the actual magnetic field configurations, it is assumed that the initial field configurations of B_r and B_φ, $b_l(t=0, r)$ and $f_l(t=0, r)$, are expressed by trigonometric functions for $1 \leq l \leq 3$ and are zero for $l \geq 4$, for simplicity. We choose an initial scale of the magnetic field, B_0, to be $B_0 = 0.9 \times 10^{11}$ G, to satisfy the condition in which ohmic dissipation dominates.

In our numerical calculation, we adopt a rather artificial form of B_r, as shown in Fig. 1. The inner boundary value of B_r is always zero [$B_r(t, R_{in}) \ll B_0$]. We also calculate the field evolution with the inner boundary condition, $B_r(t, R_{in}) \sim B_0$. In this case, we find that the Hall current terms soon dominate near the inner boundary sphere, and our numerical scheme breaks down. In our numerical method, we assume that the dissipative terms are always larger than the Hall drift terms (Section 4.1). In the opposite case, the basic equations have different characteristics and hence a different numerical scheme is necessary. Since we have limited the boundary condition to $B_r(t, R_{in}) \ll B_0$, our model describes the physical situation that the magnetic field is confined only to the crust, as some authors previously considered (Sang & Chanmugam 1987, 1990; Urpin & Muslimov 1992). Even with the restricted boundary condition, our model can partially clarify the effect of the Hall drift on the field evolution.

We also calculate the evolution without the Hall current, that is, with no toroidal magnetic field, and the results are shown in Fig. 2. In this case, the equations are linear so that we can arbitrarily scale the field strength. Fig. 2 shows the evolution of the polar surface fields as a function of time. The uppermost line indicates the evolution of the dipole field ($l = 1$). The second line represents $l = 2$ and the third line $l = 3$. They decay exponentially, with an e-folding time of $\sim 10^8$ yr, and fields with a larger l dissipate more rapidly. This result is consistent with the discussion in Section 3. For comparison, these results are shown by dotted lines in Figs 3 and 4, in which results with the Hall current included are given.

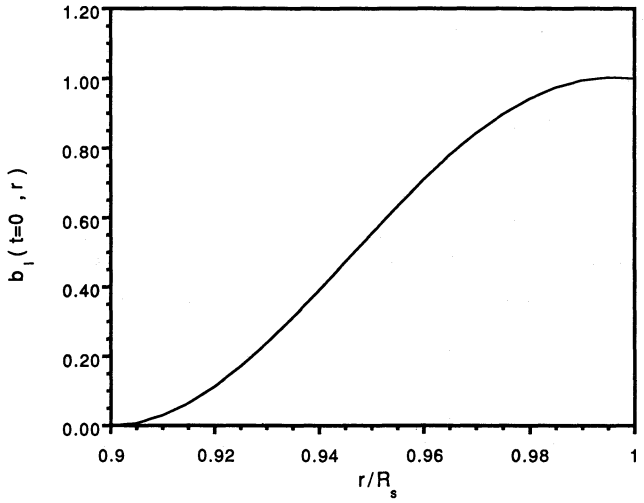

Figure 1. The initial poloidal magnetic field $b_l(t=0, r)$. The stellar surface and inner boundary of the crust correspond to $r = R_s$ and $r = 0.9\,R_s$, respectively.

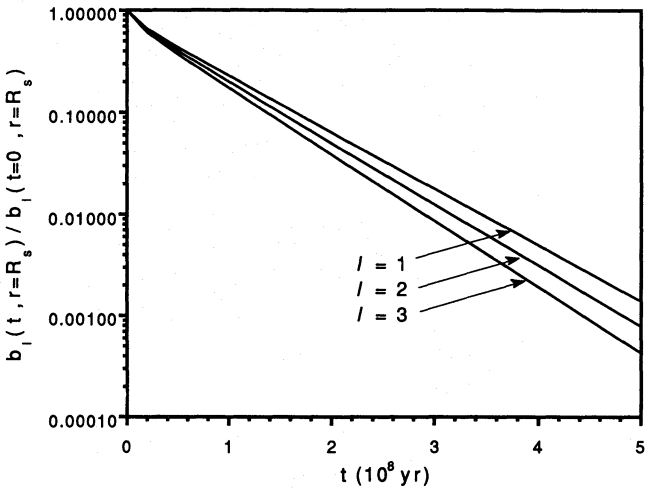

Figure 2. Magnetic field decay without the Hall current term. The ratio of the field strength to the initial value in the poloidal field at the surface is shown as a function of time in units of 100 Myr.

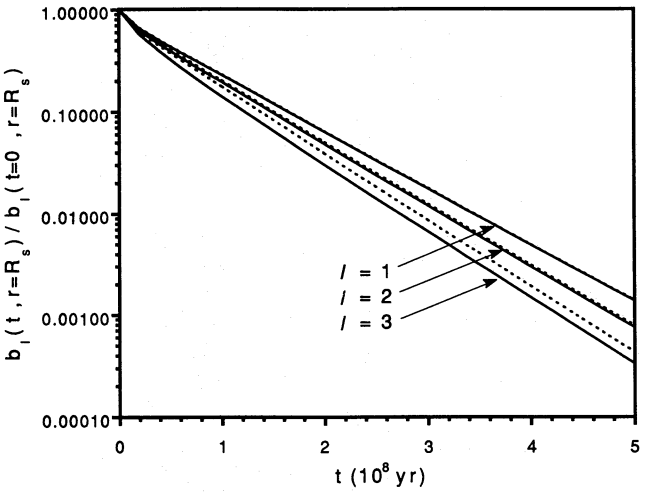

Figure 3. As Fig. 2, but with the Hall current term under the boundary condition (i) at the stellar surface. The solid lines show results with the Hall current, and the dotted lines show those without it.

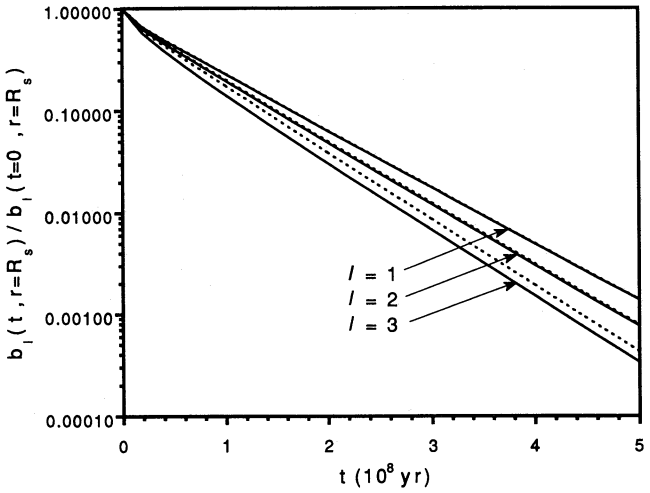

Figure 4. As Fig. 3, but under the boundary condition (ii).

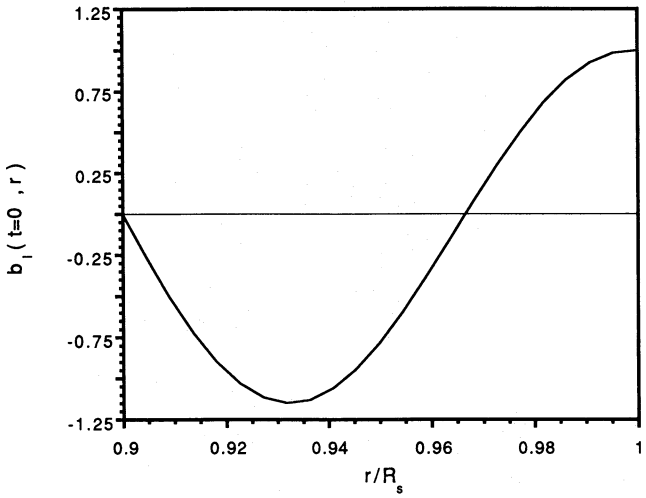

Figure 5. As Fig. 1, but for model (b). In this model, there is one loop of the field in the radial direction for each multipole field.

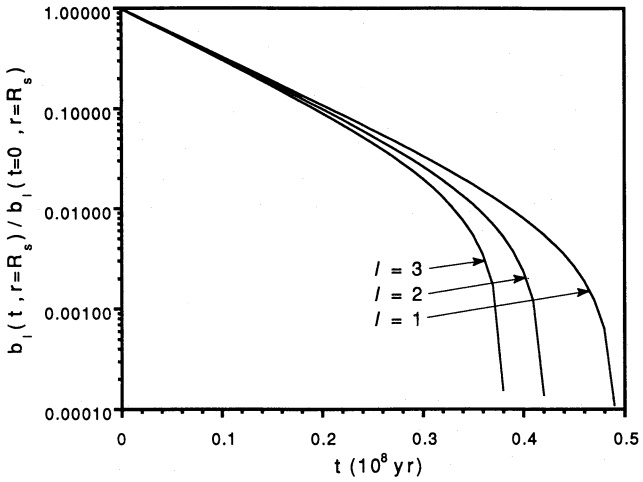

Figure 6. As Fig. 2, but for model (b).

4.2.1 *Model (a)*

We adopt two boundary conditions at the stellar surface, as discussed in Section 3.4. The results for the condition (i) are given in Fig. 3, and those for (ii) are given in Fig. 4. The initial configurations of B_φ are assumed to be single-peaked sinusoidal fields, except that $l = 1$ for the condition (ii). Since the boundary condition (ii) means that $B_\varphi \neq 0$, we use the same form as Fig. 1 for B_φ, of $l = 1$. As shown in Figs 3 and 4, the magnetic fields decay slightly faster than those without a Hall current. The reduction rate from the case without a Hall current is only a few per cent for a dipole field, and 20–30 per cent for $l = 3$. Here, we have assumed that the fields for $l > 4$ are initially zero. The higher modes are greatly affected by the Hall current term, if they exist, but they diminish the dipole field very little through mode coupling. For this initial magnetic field, therefore, the Hall current term does not effectively change the magnetic evolution, which is not different from the evolution with ohmic diffusion only.

4.2.2 *Model (b)*

We investigate another initial condition, shown in Fig. 5 for B_r. This field configuration means that the magnetic field has closed loops in the star. As for B_φ, we use the same initial form as in model (a). The results without a Hall current are shown in Fig. 6.

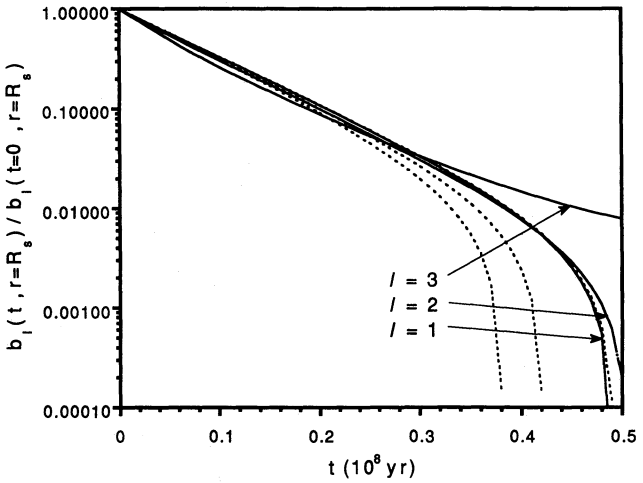

Figure 7. As Fig. 3, but for model (b).

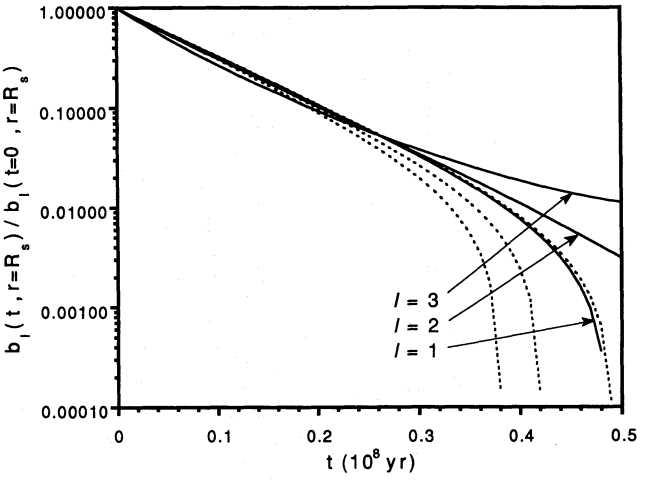

Figure 8. As Fig. 4, but for model (b).

The magnetic fields decay exponentially at first, but decay steeply beyond 30 Myr. In addition, the fields decrease 10 times faster than those in model (a). The initial fields have a node in the radial direction, and result from the combination of the positive and negative fields. With time, the negative component survives and emerges near the surface. Thus the magnetic fields at the surface decrease steeply. Fig. 6 also shows that the field with larger l dissipates more rapidly and that the dipole magnetic field survives.

The numerical solutions incorporating the Hall current effect under the boundary conditions (i) and (ii) are shown in Figs 7 and 8, respectively. In both cases, the $l=2$ and $l=3$ components show substantial changes compared with the case without Hall current (dotted line), but the dipole component does not. After 50 Myr, the $l=3$ field exceeds the dipole field by two orders of magnitude; the $l=2$ field exceeds the dipole field only slightly under boundary condition (i), but by one order of magnitude under condition (ii).

5 DISCUSSION

Magnetic field decay with the Hall current is examined for a specific magnetic configuration which is confined in the crust. Since the actual field configuration is not available, it is the purpose of this paper to demonstrate the effect of the Hall current, which seems to play a role in the evolution of the neutron star magnetic field. From the results in Section 4, the magnetic field decay depends on the configuration, but the node of the field in the radial direction (closed-loop field), as considered in model (b), seems to be important. Magnetic fields with such an initial configuration are rapidly damped and the energy of the globally aligned magnetic field is temporarily transferred to the locally disordered modes through the Hall current. In this case, we expect the magnetic field to become chaotic at its surface, where higher multipole modes dominate. Such a configuration of the neutron star may resemble that of a gamma-ray burster (Krolik 1991). In addition, we also consider the effect of the boundary conditions at the stellar surface. The difference is a factor of a few at most. If the field evolution in isolated neutron stars and that in binary systems are different, another mechanism is necessary – for example, accretion keeps the neutron star hot and decreases the conductivity.

In the numerical calculations, we assume that the dissipation term dominates during evolution, that is, $\tau_D \leq \tau_H$. The evolution equation is therefore of diffusive type, but the equation becomes non-linear (of advective type) for $\tau_D \geq \tau_H$. Since the stability of our numerical scheme is violated under such a condition, $\tau_D \geq \tau_H$. It is necessary to develop a numerical code to simulate such a case, in which the mode couplings occur quickly and the energy gradually leaks out. This occurs when strong magnetic fields ($B_s \geq 10^{12}$ G) exist near the inner boundary or throughout the crust. We expect the Hall drift to affect the evolution in a similar way, but more strongly than considered here. Further study is necessary to reach a definite conclusion.

Finally, when this paper was essentially complete, we found the paper by Goldreich & Reisenegger (1992), who discussed the importance of the Hall current as well as of ambipolar diffusion, but the latter effect is not included here. Goldreich & Reisenegger (1992) only speculated that the Hall current causes magnetic field cascades and enhances ohmic dissipation when the Hall current term dominates during evolution. In this paper, we have regarded the term as a small correction and explicitly calculated the evolutionary scenario to examine the effect, and have reached a similar conclusion to that of Goldreich & Reisenegger.

ACKNOWLEDGMENTS

We thank Professor Fumio Takahara and Professor Noriaki Shibazaki for useful discussions and encouragement. We also thank the nuclear physics group at the TMU for their assistance in calculating the Clebsch–Gordan coefficients. One of the authors (TN) is indebted in the Japan Society for Promotion of Science for Japanese Junior Scientists. This work is supported in part by the Japanese Grant-in-aid for Science Research Fund (04740131).

REFERENCES

Alpar M. A., Anderson P. W., Pines D.,Shaham J., 1984a, ApJ, 276, 325
Alpar M. A., Langer S. A., Sauls J. A., 1984b, ApJ, 284, 533
Baym G., Pethick C., Pines D., 1969a, Nat, 224, 673
Baym G., Pethick C., Pines D., 1969b, Nat, 224, 674
Blandford R. D., Applegate J. H., Hernquist L., 1983, MNRAS, 204, 1025
Chao N. C., Clark J. W., Yang C. H., 1972, Nucl. Phys. A, 179, 320
Chen F. F., 1986, Introduction to Plasma Physics & Controlled Fusion, 2nd edn. Plenum Press, New York
Ewart G. M., Guyer R. A., Greenstein G., 1975, ApJ, 202, 238
Flowers E., Itoh N., 1976, ApJ, 206, 218
Goldreich P., Reissenegger A., 1992, ApJ, 395, 250
Harrison E., 1991, MNRAS, 248, 419
Jones P. B., 1987, MNRAS, 228, 419
Jones P. B., 1988, MNRAS, 233, 875
Krolik J. H., 1991, ApJ, 373, L69
Lamb D. Q., 1992, in Tanaka Y., Koyama K., eds, Frontiers of X-ray astronomy. Universal Academy Press, Tokyo, p. 33
Lamb H., 1883, Phil. Trans. R. Soc. Lond., 174, 519
Lyne A. G., Manchester R. N., Taylor J. H., 1985, MNRAS, 213, 613
Manchester R. N., Taylor J. H., 1977, Pulsars. W. H. Freeman & Co., San Francisco
Murakami T. et al., 1988, Nat, 335, 234
Narayan R., Ostriker J. P., 1990, ApJ, 352, 222
Nomoto K., Tsuruta S., 1987, ApJ, 312, 711
Ostriker J. P., Gunn J. E., 1969, ApJ, 157, 1395
Pines D., Alpar M. A., 1985, Nat, 316, 27
Sang Y., Chanmugam G., 1987, ApJ, 323, L61
Sang Y., Chanmugan G., 1990, ApJ, 363, 597
Shapiro S. L., Teukolsky S. A., 1983, Black Holes, White Dwarfs, & Neutron Stars. Wiley-Interscience, New York
Shibazaki N., Murakami T., Shaham J., Nomoto K., 1989, Nat, 342, 656
Taam R. E., van den Heuvel E. P. J., 1986, ApJ, 305, 235
Urpin V. A., Muslimov A. G., 1992, MNRAS, 256, 261
Urpin V. A., Levshakov S. A., Yakovlev D. G., 1986, MNRAS, 219, 703
Verbunt F., Wijers R. A. M. J., Burm H. M. G., 1990, A&A, 234, 195
Wendell C. E., Van Horn H. M., Sargent D., 1987, ApJ, 313, 284

APPENDIX

We summarize here the characteristics of Legendre polynomials, and derive the integrals (31) using Legendre associated functions and spherical harmonics.

The definition of a Legendre polynomial is

$$P_l(z)=\frac{1}{2^l l!}\frac{\mathrm{d}^l}{\mathrm{d}z^l}(z^2-1)^l, \tag{A1}$$

and it satisfies the differential equation

$$\frac{1}{\sin\theta}\frac{\partial}{\partial\theta}\left[\sin\theta\frac{\partial P_l(\cos\theta)}{\partial\theta}\right]=-l(l+1)P_l(\cos\theta). \tag{A2}$$

We apply this differential equation repeatedly to the magnetic field and time evolution functions, and obtain the relations (24), (25), (27) and (28).

In order to calculate (31), we introduce Legendre associated functions and spherical harmonics. Legendre associated functions are expressed by Legendre polynomials as

$$P_l^{|m|}(z)=(1-z^2)^{|m|/2}\frac{\mathrm{d}^{|m|}}{\mathrm{d}z^{|m|}}P_l(z). \tag{A3}$$

Further, the definition of spherical harmonics is

$$Y_l^m(\theta,\phi)=(-1)^{(m+|m|)/2}\sqrt{\frac{2l+1}{4\pi}\frac{(l-|m|)!}{(l+|m|)!}}P_l^{|m|}(\cos\theta)\,\mathrm{e}^{\mathrm{i}m\phi}. \tag{A4}$$

One can write the definition of the Glebsch–Gordon coefficient as

$$\int Y^{*m_3}_{l_3}\, Y^{m_2}_{l_2}\, Y^{m_1}_{l_1}\, \mathrm{d}\Omega = \sqrt{\frac{(2l_1+1)(2l_2+1)}{4\pi(2l_3+1)}}\, C(l_1 l_2 l_3; m_1 m_2 m_3)\, C(l_1 l_2 l_3; 000), \tag{A5}$$

where $\mathrm{d}\Omega = \sin\theta\, \mathrm{d}\theta\, \mathrm{d}\phi$ and $C(l_1 l_2 l_3; m_1 m_2 m_3)$ is the Clebsch–Gordan coefficient. Using the relations (A3) and (A4) we obtain

$$Y^{*1}_{l_3}(\theta,\phi)\, Y^{1}_{l_2}(\theta,\phi)\, Y^{0}_{l_1}(\theta,\phi) = \frac{\sqrt{(2l_1+1)(2l_2+1)(2l_3+1)}}{(4\pi)^{3/2}} \sqrt{\frac{(l_2-1)!\,(l_3-1)!}{(l_2+1)!\,(l_3+1)!}}\, P_{l_1}(z)(1-z^2)\, \frac{\partial P_{l_2}(z)}{\partial z}\, \frac{\partial P_{l_3}(z)}{\partial z} \tag{A6}$$

where $z = \cos\theta$. The integral over $\mathrm{d}\Omega$ yields

$$\begin{aligned}\int Y^{*1}_{l_3}\, Y^{1}_{l_2}\, Y^{0}_{l_1}\, \mathrm{d}\Omega &= \frac{\sqrt{(2l_1+1)(2l_2+1)(2l_3+1)}}{\sqrt{l_2(l_2+1)\,l_3(l_3+1)}}\, \frac{2\pi}{(4\pi)^{3/2}} \int_{-1}^{1} P_{l_1}(\cos\theta)\, \frac{\partial P_{l_2}(\cos\theta)}{\partial\theta}\, \frac{\partial P_{l_3}(\cos\theta)}{\partial\theta}\, \mathrm{d}(\cos\theta) \\ &= \sqrt{\frac{(2l_1+1)(2l_2+1)}{4\pi(2l_3+1)}}\, C(l_1 l_2 l_3; 001)\, C(l_1 l_2 l_3; 000).\end{aligned} \tag{A7}$$

Thus we have obtained the integral S in equation (24) as follows:

$$\int_{-1}^{1} P_{l_1}\, \frac{\partial P_{l_2}}{\partial\theta}\, \frac{\partial P_{l}}{\partial\theta}\, \mathrm{d}(\cos\theta) = \frac{2}{2l+1}\, \sqrt{l_2(l_2+1)\,l(l+1)}\; C(l_1 l_2 l; 001)\, C(l_1 l_2 l; 000). \tag{A8}$$

In a similar way, we obtain the expression for S' by substituting l_3 and l.